05

CM-2A molybdenum alloy sheet rolling crystallographic texture evolution prediction using modelling

© V.P. Tyutin, O.A. Krymskaya, M.G. Isaenkova

National Research Nuclear University „MEPhI“, Moscow, Russia
E-mail: vp.tyutin@gmail.com

Received December 16, 2025
Revised January 12, 2026
Accepted January 12, 2026

Modeling of the crystallographic texture in the CM-2A molybdenum alloy was performed for various rolling schemes. Based on experimental data, the ratio of the critical shear stresses in the $\{110\}\langle 111\rangle$ and $\{112\}\langle 111\rangle$ slip systems was determined $\tau_{(110)}/\tau_{(112)} = 1.1-1.2$ at which the difference between the experimental and calculated grain orientation distribution functions is minimal. It is shown that the type of active slip systems changes during unidirectional rolling, while one slip-system type predominates during cross rolling.

Keywords: molybdenum, crystallographic texture, cold rolling, modeling, Taylor model.

DOI: 10.61011/TPL.2026.05.63283.20603

Molybdenum and molybdenum alloys are among most highly-demanded structural materials for high-temperature applications due to a combination of high melting temperature (2623 °C), low thermal expansion coefficient, high thermal conductivity and creep resistance [1,2]. TZM (Mo−0.5Ti−0.08Zr−0.02C) and CM-2A (a domestic alloy with identical composition) alloys are the most widely used molybdenum-based alloys for aerospace, nuclear and electronic industries, in particular, for fabrication of heat screen components, dies, and structural components operating at 1200−1800 °C.

Crystallographic texture formed during thermomechanical treatment is one of the key factors that define performance of semi-finished molybdenum alloy sheet products. Sharp rolling texture causes distinct anisotropy of stress-strain properties. For the TZM and CM-2A alloys this is a serious issue because high anisotropy can account for separations and brittle fracture under thermomechanical loading [3]. In particular, forming of products from molybdenum sheets leads to earing, which is caused by crystallographic texture characteristics and is indicative of nonuniform plastic deformation [4]. Therefore understanding of texture formation patterns and development of texture control methods on the basis of these patterns are important to improve the quality of molybdenum alloy products.

Formation of deformation texture of metals with body-centered cubic (BCC) lattice is defined by the action of the $\{110\}\langle 111\rangle$, $\{112\}\langle 111\rangle$ and $\{123\}\langle 111\rangle$ slip systems, however, critical shear stresses in them depend on rolling temperature [3]. It is shown experimentally that in ultrapure molybdenum the Peierls barrier for dislocations in the $\{112\}\langle 111\rangle$ system is lower than for $\{110\}\langle 111\rangle$ (690 MPa and 870 MPa, respectively) [5], which is indicative of an easier activation of the $\{112\}\langle 111\rangle$ system. *Ab initio* calculations of the Peierls barriers for hard-melting metals with BCC structure such as W, Nb, Mo and Ta show that $\{110\}\langle 111\rangle$ remains as the most energetically favorable slip system [6].

It is the slip system activation nonuniformity that causes earing. The presence of the $\{001\}\langle 110\rangle$ type sharp cubic texture in a sheet reduces the likelihood of activation of the $\{110\}\langle 111\rangle$ type slip systems, therefore plastic flow of metal in rolling direction and transverse direction is hindered. Whereas at 45° to the rolling direction, the slip is possible in the $\{110\}\langle 111\rangle$ and $\{112\}\langle 111\rangle$ systems, causing protrusions — ears. To avoid earing, uniform distribution of the $\{110\}$ normals in the sheet plane shall be achieved [4].

Computer-aided simulation on the basis of crystallographic laws of plastic deformation is an effective tool for detecting texture formation patterns during rolling and for optimizing deformation parameters. The Taylor model is the most widely used approach to texture simulation during plastic deformation and assumes that the macroscopic deformation tensor is equal for all grains of the polycrystal of interest [7]. This model determines reorientation of some crystallites, predicts texture formation, demonstrates good coincidence of theoretical and experimental data [9] for metals with a cubic crystal system [8], and thus can be used as an effective tool for deformation scheme analysis by texture.

This study intends to adapt the plastic deformation model in MTEX as applicable to CM-2A alloy and to verify the model by the experimental cold rolling results for molybdenum sheets.

CM-2A test samples were prepared via cold rolling of original sample 0 with a thickness of 0.8 mm longitudinally along the initial rolling direction (RD_0) (sample 1), crosswise while maintaining RD_0 (sample 2), and longitudinally (sample 3) and crosswise (sample 4) at 45° to RD_0. Rolling was performed at the deformation rate $\dot{\varepsilon} = 2-5\,s^{-1}$ until the shrinkage $\varepsilon = 75\,\%$ was achieved, which corresponds to the true degree of deformation $\epsilon = 1.39$. Structural

state of rolled sheets was evaluated by diffraction spectra measured using the D8 Discover X-ray diffractometer fitted with the LynxEye linear detector and CuK_α tube. X-ray diffraction spectra from sample surfaces (normal direction, ND) indicate that there is a single BCC Mo phase. The measured spectra (Figure 1) were used to determine the angular positions of lines (200), (220) and (222) for the measurement of incomplete direct pole figures to be used for reconstruction of the orientation distribution function (ODF). The main texture components observed in all samples: $\{001\}\langle 110\rangle$, $\{001\}\langle 100\rangle$ and $\langle 111\rangle \| \mathrm{ND}$ (γ-fiber). ODF was used to evaluate the proportion of texture components [10]:

$$V = \int_{c}^{c+r} f(g)dg,$$

where c is the position of the center of a texture component (in degrees), r is the apex angle of cone in the Euler angle space, within which summation takes place, $r = 5^\circ$.

Simulation error was determined by coincidence of the calculated ODF $f_{mod}(g)$ and experimental ODF $f_{exp}(g)$ in statistically significant areas $\big(f(g) > 0.5\big)$:

$$E = \frac{\int |f_{exp}(g) - f_{mod}(g)|dg}{\int f_{exp}(g)dg}.$$

MTEX open-source software was used for cold rolling simulation.

Rolling conditions were set by the deformation tensor $F_\parallel$. Crosswise rolling involved deformation simulation with alternating deformation tensors of direct rolling $F_\parallel$ and transverse rolling $F_\perp$. Chosen rolling conditions are a simplification that doesn't account for nonuniform deformation over the sheet thickness, however, are permitted for the purpose of this work because they allow a rolling direction change to be set for simulation.

$$F_\parallel = \epsilon_i \cdot \begin{bmatrix} 1 & 0 & 0 \\ 0 & 0 & 0 \\ 0 & 0 & -1 \end{bmatrix}, \quad F_\perp = \epsilon_i \cdot \begin{bmatrix} 0 & 0 & 0 \\ 0 & 1 & 0 \\ 0 & 0 & -1 \end{bmatrix},$$

where ϵ_i is the true degree of deformation per pass.

Texture of rolled samples with various deformation schemes is shown in Figure 1 in the form of ODF cross-sections at $\varphi_2 = 45^\circ$. Experimental results were used for model verification and choosing the critical shear stress ratio τ. Texture formation was simulated by the deformation schemes corresponding to the schemes for samples 1 to 4 with $\tau_{(110)}/\tau_{(112)}$ varied from 0.5 to 2 (Figure 2, *a*). Consideration of the $\{123\}\langle 111\rangle$ slip systems doesn't result in a change of texture at $\tau_{(123)}$ ranging from $0.5\tau_{(112)}$ to $3\tau_{(112)}$ when the shrinkage of 1.39 is reached, and this slip system is not included in further calculations. The greatest simulation error is observed for longitudinal rolling cases, which can be attributed to the aspects of error calculation: for a sharp texture (typical of crosswise rolling — samples 2 and 4), the error is small because only statistically significant ODF regions $(f(g) > 0.5)$ are included in the calculation. For longitudinal rolling, texture smearing is observed, i. e. Euler angle regions are formed where the residual $|f_{exp}(g) - f_{mod}(g)|$ is small, but the proportion of such regions is quite large. Nevertheless, they also contain typical minima corresponding to the best coincidence between the experimental and simulated ODFs.

The best coincidence between the simulation and experimental results is achieved with $\tau_{(110)}/\tau_{(112)} = 1.1-1.2$, which agrees qualitatively with the results obtained in [5]. Deviation from the Peierls barrier ratio $\sigma_{(110)}/\sigma_{(112)} \approx 1.26$ reported in the literature can be explained by the fact that the literature data is given for high-purity Mo, and this work deals with the CM-2A alloy [5].

For simulation of rolling with the chosen $\tau_{(110)} = 1.1\tau_{(112)}$, growth of the γ-fiber component was detected at the initial stage during deformation according to all schemes (Figure 2, *b*). Differences in further mode of formation of this component depend on activities of the $\{110\}\langle 111\rangle$ ($a_{\{110\}\langle 111\rangle}$) and $\{112\}\langle 111\rangle$ ($a_{\{112\}\langle 111\rangle}$) slip systems. In samples 1 and 2 rolled longitudinally and crosswise relative to RD_0, $a_{\{110\}\langle 111\rangle}$ is limited by a low Schmid factor for this system in grains with the $\{001\}\langle 110\rangle$ texture component, therefore at the initial deformation stage $a_{\{110\}\langle 111\rangle} < a_{\{112\}\langle 111\rangle}$ (Figure 3, *a*, *b*). However, longitudinal rolling (sample 1) causes smearing of the $\{001\}\langle 110\rangle$ component, facilitating the activization of the slip in the $\{110\}\langle 111\rangle$ system (Figure 2, *b*), and formation of the γ-fiber stops when $\epsilon = 0.7-0.8$ is reached. Crosswise rolling (sample 2), on the contrary, prevents smearing of $\{110\}\langle 111\rangle$, and $a_{\{110\}\langle 111\rangle}$ decreases monotonically with simultaneous monotonic growth of the γ-fiber components (Figure 2, *b*).

Samples 3 and 4 rolled at 45° relative to RD_0 are characterized by a greater $a_{\{110\}\langle 111\rangle}$. This is explained by the fact that when the rolling direction is changed, the $\{001\}\langle 110\rangle$ component becomes $\{001\}\langle 100\rangle$, for which the Schmid factor of the $\{110\}\langle 111\rangle$ system doesn't tend to zero any longer. Therefore, crosswise rolling (sample 4) is accompanied by the growth of $a_{\{110\}\langle 111\rangle}$ and increase in the proportion of the γ-fiber. Longitudinal rolling (sample 3), as for sample 1, is also accompanied by ending of formation of the γ-fiber component and reduction of $a_{\{110\}\langle 111\rangle}$ when $\epsilon = 0.7-0.8$ is reached.

Mean cumulative shear in grains of various texture components was determined using the simulation data: ratios for the γ-fiber, $\{001\}\langle 100\rangle$ and $\{001\}\langle 110\rangle$ were $(1.52-1.60):(1.13-1.16):1$, respectively. This proves that grains forming the γ-fiber are the most hard-drawn, and grains of the $\{001\}\langle 110\rangle$ component are subjected to lower deformation due to suppression of the $\{110\}\langle 111\rangle$ slip systems.

Thus, the following conclusions were made by comparing the experimental and theoretical data.

1. The Taylor plastic deformation model was used for predicting the crystallographic texture of cold rolling of

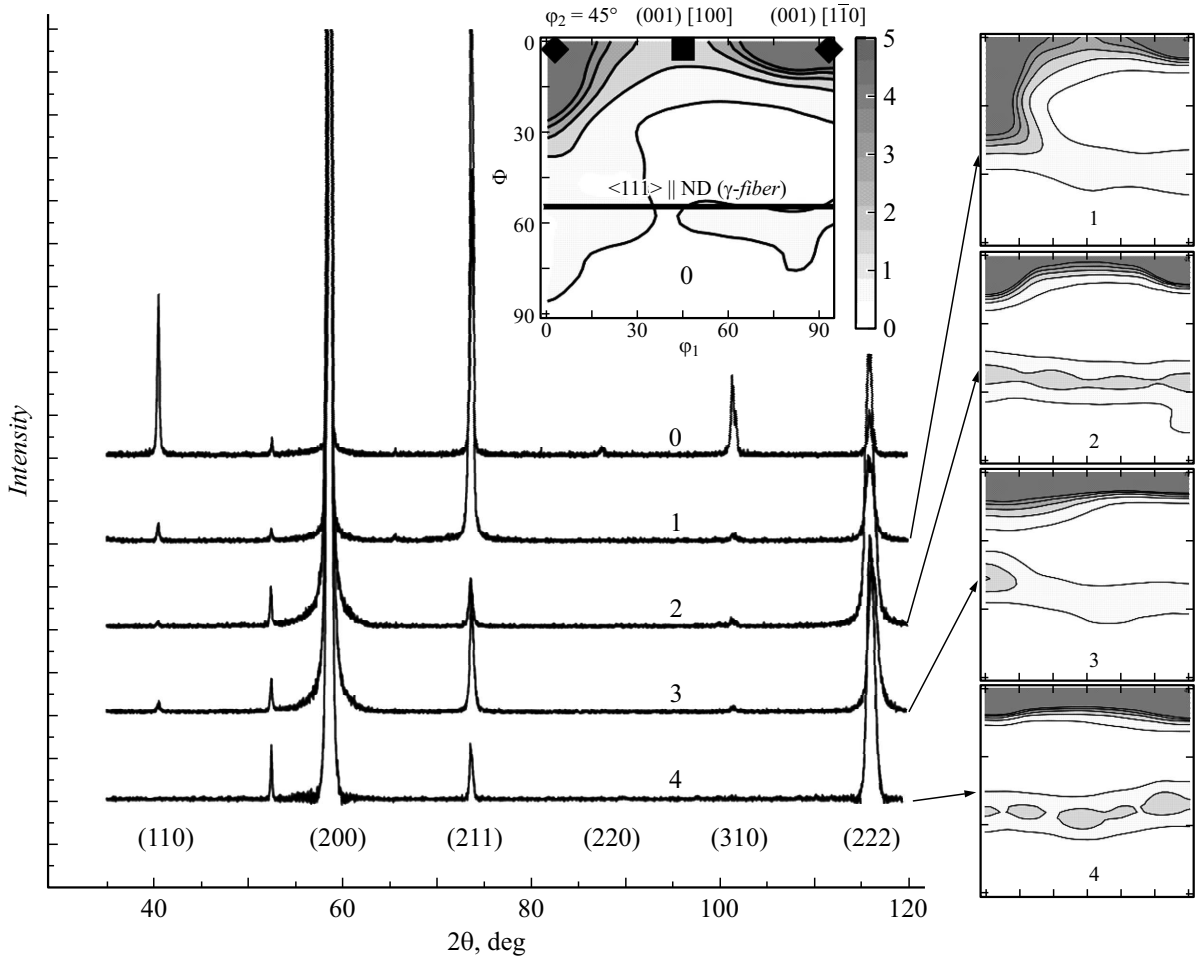

Figure 1. X-ray diffraction spectra (reflecting plane indices are shown in brackets) and ODF cross-sections for $\varphi_2 = 45^\circ$ of the studied test samples (numbers 0 to 4 are sample numbers). ND — normal direction.

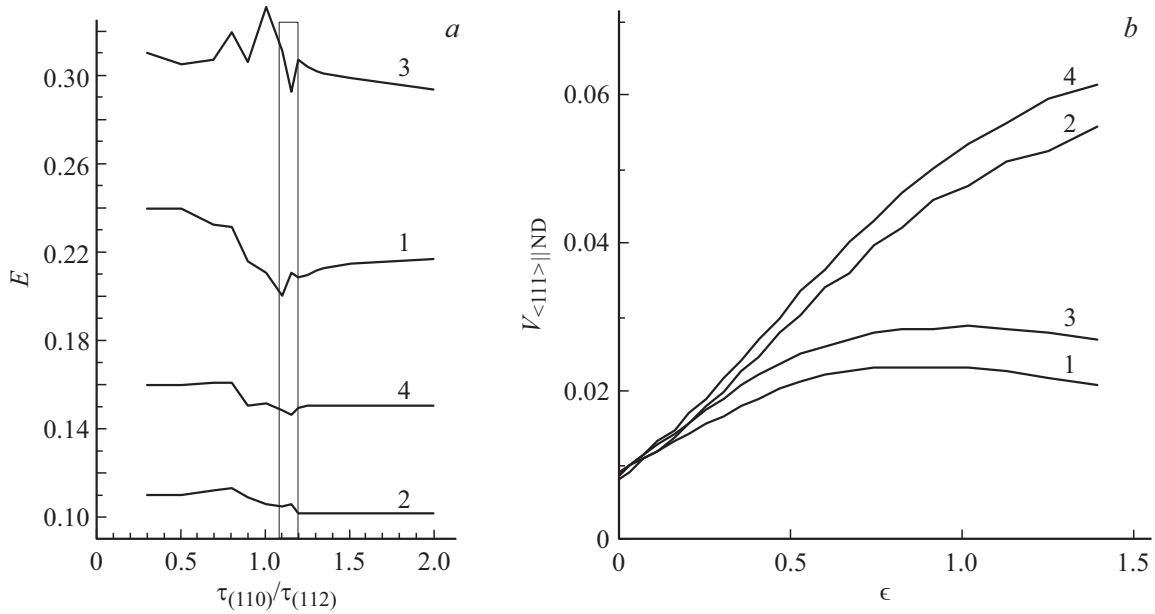

Figure 2. Simulation of the plastic deformation of molybdenum sheets. *a* — variation of the simulation error E with varying ratio of critical shear stresses $\tau_{(110)}/\tau_{(112)}$. The least error interval of $\tau_{(110)}/\tau_{(112)}$ is highlighted. *b* — proportion of component $V_{\langle 111\rangle\|\mathrm{ND}}$ (γ-fiber) vs. the true degree of deformation. 1 to 4 are sample numbers.

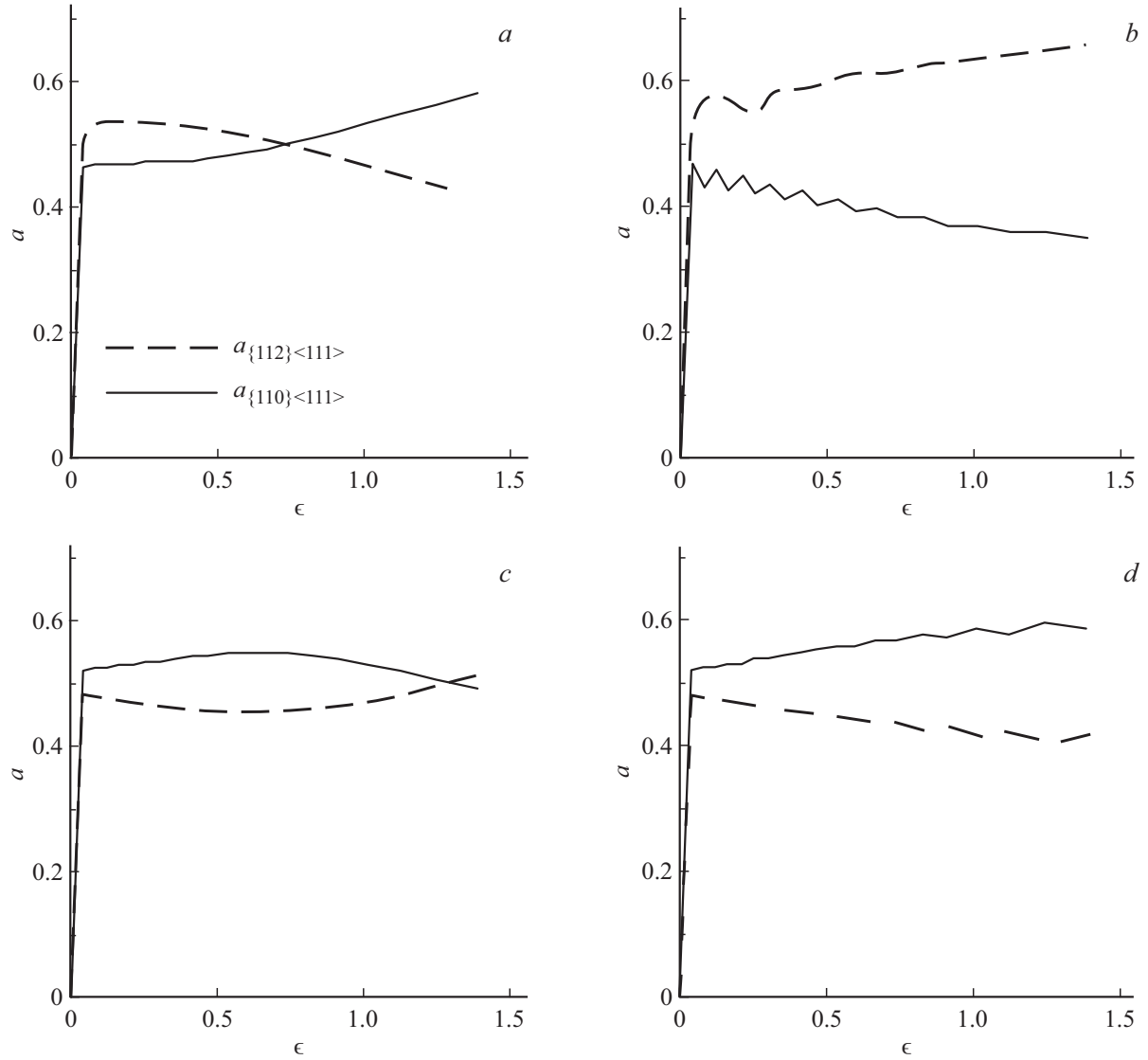

Figure 3. Simulation of the plastic deformation of molybdenum sheets. $a-d$ — activities of the $a_{\{112\}\langle 111\rangle}$ and $a_{\{110\}\langle 111\rangle}$ slip systems vs. the true degree of deformation ϵ for samples 1 to 4, respectively.

the CM-2A sheets. It has been found that when the ratio of the critical shear stresses τ_{110} and τ_{112} was varied for the $\{110\}\langle 111\rangle$ and $\{112\}\langle 111\rangle$ slip systems, respectively, the best coincidence of the theoretical and experimental functions of grain distribution over orientations was reached at $\tau_{110}/\tau_{112} = 1.1-1.2$, in this case qualitative and quantitative coincidence was observed for all rolling schemes discussed in the work. The findings make it possible to recommend the developed model for various cold deformation flow charts for the Ts-M-2A with various grain orientations.

2. It is shown experimentally and theoretically that longitudinal and crosswise cold rollings of the CM-2A molybdenum alloy sheets with the $\{001\}\langle 110\rangle$ crystallographic texture relative to the initial rolling direction result in enhancement of this component at a shrinkage of 1.39. When the rolling direction is changed to 45° relative to RD_0, axial texture with the $\langle 001\rangle \| ND$ axis can be obtained, thus providing the isotropy in the sheet plane, which is necessary for further forming, compared with the sharp $\{001\}\langle 110\rangle$ crystallographic texture.

3. It has been found that crosswise rolling to a degree of deformation of 1.39 caused an increase in the proportion of the $\langle 111\rangle \| ND$ component, while formation of the component stopped during longitudinal rolling when a degree of deformation of $0.7-0.8$ was reached, which was associated with relaxation of activity of the $\{112\}\langle 111\rangle$ slip systems during rolling in the initial direction and of the $\{110\}\langle 111\rangle$ systems during rolling at 45° to this direction.

Funding

This study was performed as part of the Priority 2030 academic leadership program (project SP-1).

Conflict of interest

The authors declare no conflict of interest.

References

[1] R. Su, L. Liu, J.H. Perepezko, Int. J. Refract. Met. Hard Mater., **113**, 106199 (2023). DOI: 10.1016/j.ijrmhm.2023.106199
[2] P.M. Cheng, C. Yang, P. Zhang, J.Y. Zhang, H. Wang, J. Kuang, J. Sun, J. Mater. Sci. Technol., **130**, 53 (2022). DOI: 10.1016/j.jmst.2022.04.043
[3] L.A.I. Kestens, H. Pirgazi, Mater. Sci. Technol., **32**, 1303 (2016). DOI: 10.1080/02670836.2016.1231746
[4] K.K. Park, J.H. Cho, H.N. Han, H.C. Lee, K.H. Oh, Key Eng. Mater., **233-236**, 567 (2003). DOI: 10.4028/www.scientific.net/KEM.233-236.567
[5] L. Hollang, D. Brunner, A. Seeger, Mater. Sci. Eng. A, **319**, 233 (2001). DOI: 10.1016/S0921-5093(01)01002-4
[6] X.C. Zhang, S. Cao, L.J. Zhang, R. Yang, Q.M. Hu, J. Mater. Res. Technol., **22**, 3413 (2023). DOI: 10.1016/j.jmrt.2022.12.162
[7] U.F. Kocks, C.N. Tomé, H.R. Wenk, *Texture and anisotropy: preferred orientations in polycrystals and their effect on materials properties* (Cambridge University Press, 2000), p. 390–407.
[8] J. Galán-López, L.A. Kestens, Metallurg. Mater. Trans. A, **49**, 5745 (2018). DOI: 10.1007/s11661-018-4869-8
[9] O.A.Krymskaya, M.G.Isaenkova, R.A.Minushkin, Yu.A.Romanova, V.P.Tyutin, S.V.Danilov, Metally, No 2, 24 (2025).(in Russian) DOI: 10.31857/S0869573325022433
[10] F. Bachmann, R. Hielscher, H. Schaeben, Solid State Phenomena, **160**, 63 (2010). DOI: 10.4028/www.scientific.net/SSP.160.63

Translated by E.Ilyinskaya